

Preliminary Study of Realistic Blast Impact on Cultured Brain Slices

**by Thuvan Piehler, Rohan Banton, Lars Piehler, Richard Benjamin,
Ray Sparks, Marquitta Smith, and Ben A Bahr**

ARL-TR-7197

April 2015

NOTICES

Disclaimers

The findings in this report are not to be construed as an official Department of the Army position unless so designated by other authorized documents.

Citation of manufacturer's or trade names does not constitute an official endorsement or approval of the use thereof.

Destroy this report when it is no longer needed. Do not return it to the originator.

Army Research Laboratory

Aberdeen Proving Ground, MD 21005-5066

ARL-TR-7197**April 2015**

Preliminary Study of Realistic Blast Impact on Cultured Brain Slices

**Thuvan Piehler, Rohan Banton, Lars Piehler, Richard Benjamin,
and Ray Sparks**

Weapons and Materials Research Directorate, ARL

**Marquitta Smith and Ben A Bahr
Biotechnology Research and Training Center
University of North Carolina - Pembroke**

| REPORT DOCUMENTATION PAGE | | | Form Approved OMB No. 0704-0188 | | |
|--|-----------------------------|------------------------------|--|--|---|
| Public reporting burden for this collection of information is estimated to average 1 hour per response, including the time for reviewing instructions, searching existing data sources, gathering and maintaining the data needed, and completing and reviewing the collection information. Send comments regarding this burden estimate or any other aspect of this collection of information, including suggestions for reducing the burden, to Department of Defense, Washington Headquarters Services, Directorate for Information Operations and Reports (0704-0188), 1215 Jefferson Davis Highway, Suite 1204, Arlington, VA 22202-4302. Respondents should be aware that notwithstanding any other provision of law, no person shall be subject to any penalty for failing to comply with a collection of information if it does not display a currently valid OMB control number. PLEASE DO NOT RETURN YOUR FORM TO THE ABOVE ADDRESS. | | | | | |
| 1. REPORT DATE (DD-MM-YYYY) April 2015 | | 2. REPORT TYPE Final | | 3. DATES COVERED (From - To) 4-7 March 2014 | |
| 4. TITLE AND SUBTITLE Preliminary Study of Realistic Blast Impact on Cultured Brain Slices | | | 5a. CONTRACT NUMBER | | |
| | | | 5b. GRANT NUMBER | | |
| | | | 5c. PROGRAM ELEMENT NUMBER | | |
| 6. AUTHOR(S) Thuvan Piehler, Rohan Banton, Lars Piehler, Richard Benjamin, Ray Sparks, Marquitta Smith, and Ben A Bahr | | | 5d. PROJECT NUMBER DSI FY13 | | |
| | | | 5e. TASK NUMBER | | |
| | | | 5f. WORK UNIT NUMBER | | |
| 7. PERFORMING ORGANIZATION NAME(S) AND ADDRESS(ES) U.S. Army Research Laboratory ATTN: RDRL-WML-C Aberdeen Proving Ground, MD 21005-5066 | | | 8. PERFORMING ORGANIZATION REPORT NUMBER ARL-TR-7197 | | |
| 9. SPONSORING/MONITORING AGENCY NAME(S) AND ADDRESS(ES) | | | 10. SPONSOR/MONITOR'S ACRONYM(S) | | |
| | | | 11. SPONSOR/MONITOR'S REPORT NUMBER(S) | | |
| 12. DISTRIBUTION/AVAILABILITY STATEMENT Approved for public release; distribution is unlimited. | | | | | |
| 13. SUPPLEMENTARY NOTES | | | | | |
| 14. ABSTRACT Traumatic brain injury (TBI) is frequently caused by blasts that trigger a series of neuronal biochemical changes. Diagnosis of mild TBI caused by blast is challenging, since the damage to brain tissue progresses slowly over time. It is largely unknown how structural damage at tissue level from blast loading impact affects functional activity at variable time scales after the TBI event. This report describes the experimental approach and preliminary results of our study of cultured hippocampal brain slices impacted by explosively generated blast waves with single or multiple impacts in water. The initial results showed that a single blast had no effect on the immunoreactivity level of GluR1, an integral membrane protein belonging to the glutamate-gated ion channel family, whereas a triple blast insult caused a significant reduction in the GluR1 synaptic marker compared to submerged control slices. This might be an indication of a dose-dependent effect and warrants further investigation with hippocampal slice samples to better understand blast-induced brain damage. | | | | | |
| 15. SUBJECT TERMS RDX spheres, organotypic cultures of hippocampus, small scale blast, aquarium test, high-speed imaging | | | | | |
| 16. SECURITY CLASSIFICATION OF: | | | 17. LIMITATION OF ABSTRACT UU | 18. NUMBER OF PAGES 36 | 19a. NAME OF RESPONSIBLE PERSON Thuvan Piehler |
| a. REPORT Unclassified | b. ABSTRACT Unclassified | c. THIS PAGE Unclassified | | | 19b. TELEPHONE NUMBER (Include area code) (410) 278-0319 |

Contents

| | |
|--|-----------|
| List of Figures | iv |
| List of Tables | v |
| Acknowledgments | vi |
| 1. Introduction | 1 |
| 2. Objective | 1 |
| 3. Experimental Setup | 1 |
| 3.1 The Aquarium Setup | 1 |
| 3.2 Explosive Charges | 3 |
| 3.3 Pressure Sensors and Holder | 4 |
| 3.4 Experimental Arrangement | 5 |
| 3.5 Tissue Experimental Procedures | 6 |
| 3.5.1 Organotypic Cultures of Hippocampus | 6 |
| 3.5.2 Blast Insult Procedure in Hippocampal Slice Cultures | 7 |
| 3.5.3 Harvesting Hippocampal Slice Samples for Immunoblot Analysis | 8 |
| 4. Results and Discussion | 9 |
| 4.1 High-Speed Imaging Record | 9 |
| 4.2 Experimental Pressure Measurements | 12 |
| 4.3 Modeling and Simulation of Blast-Generated Pressure | 14 |
| 4.4 Assessment of the GluR1 Synaptic Marker in 48-h Post-Blast Samples | 23 |
| 5. Summary | 24 |
| 6. References | 26 |
| List of Symbols, Abbreviations, and Acronyms | 27 |
| Distribution List | 28 |

List of Figures

| | | |
|---------|--|----|
| Fig. 1 | The aquarium tank..... | 2 |
| Fig. 2 | Cultured tissue samples submerged in the aquarium tank..... | 2 |
| Fig. 3 | Spherical RDX charge-matching hemispherical charges (left) and a fully assembled 1.7-g spherical charge (right)..... | 3 |
| Fig. 4 | PCB pressure gauge arrangement..... | 4 |
| Fig. 5 | Free-field pencil gauge arrangement | 4 |
| Fig. 6 | Explosive charge arrangement..... | 5 |
| Fig. 7 | Experimental arrangement..... | 5 |
| Fig. 8 | View from the perspective of the Photron Fastcam SA5 high-speed camera | 6 |
| Fig. 9 | The organotypic hippocampal slice culture..... | 7 |
| Fig. 10 | Cultured brain slice samples submerged in medium ready for testing..... | 8 |
| Fig. 11 | The blast wave arrival images from $t = 0$ to $t = 0.30$ ms..... | 10 |
| Fig. 12 | High-speed images of the blast wave arrival images from $t = 0.30$ ms to $t = 0.65$ ms after the initiation..... | 11 |
| Fig. 13 | A typical side-on pressure-time history signature recorded in air..... | 13 |
| Fig. 14 | A typical head-on pressure-time history signature recorded in water..... | 13 |
| Fig. 15 | Numerical blast simulation setup. Test sample packs Nos. 1 and 2 were placed 180 mm from the tank front inner wall. The distances from the RDX charges to the tank front wall were 125 mm and 150 mm, respectively. Tank wall thickness was 20 mm..... | 15 |
| Fig. 16 | a) Pressure contours from RDX air blast initiated from standoff distance of 125 mm from tank front wall. b) Pressure history for tracer particle 1 located (0 cm, -0.1cm) on the tank front wall. | 17 |
| Fig. 17 | a) Pressure contours propagating across the tank wall (standoff 125 mm). b) Pressure histories for tracer particle 2 located (0 cm, 1.91 cm) on inner tank wall..... | 17 |
| Fig. 18 | Pressure waves propagating across the sample packs with tracers 3–9 identified (Initiated standoff 125 mm) | 18 |
| Fig. 19 | a) Pressure histories at tracer locations 3 and 4 located in sample pack No. 1; b) pressure histories at tracer locations 7 and 8 located in sample pack No. 2 (standoff distance 125 mm)..... | 19 |
| Fig. 20 | a) Pressure histories at tracer location 5; b) pressure histories at tracer location 9; c) pressure histories at tracer 6 located between sample packs Nos. 1 and 2. (Standoff 125 mm). | 20 |
| Fig. 21 | Comparison of experiment and calculation of pressure-time history signature recorded in water from aquarium experiment..... | 21 |

| | | |
|---------|--|----|
| Fig. 22 | Pressure waves propagating across the sample packs with tracers 3–9 identified. Explosive standoff was at 150 mm from the front of the aquarium. | 22 |
| Fig. 23 | a) Pressure histories at tracer locations 3 and 4 located in sample pack No. 1; b) pressure histories at tracer locations 7 and 8 located in sample pack No. 2 | 22 |
| Fig. 24 | a) Pressure histories at tracer location 5; b) pressure histories at tracer location 9; c) pressure histories at tracer 6 located between sample packs Nos. 1 and 2 | 23 |
| Fig. 25 | GluR1 is markedly reduced in response to a triple blast insult. OHSC's exposed to a single blast insult did not demonstrate a change in the post-synaptic marker GluR1. Triple blast shockwaves greatly reduced the level of GluR1. ANOVA $p=0.0009$ (Posthoc test *** "($p < 0.001$)). | 24 |

List of Tables

| | | |
|---------|---|----|
| Table 1 | Hemispherical charge weight..... | 3 |
| Table 2 | Peak incident (head-on) experimental pressures inside the tank | 14 |
| Table 3 | Tracer location and peak pressure at 325-mm standoff distance from the charge to the sample | 16 |
| Table 4 | Peak pressures generated by simulation at the entrance, inside and back wall of sample packs | 16 |

Acknowledgments

The US Army Research Laboratory (ARL) Director of the US Army Research Development and Engineering Command (RDECOM) funded this effort through the FY13 Director's Strategic Initiatives (DSI) Program.

The authors would like to thank Dr. Frederick Gregory (Army Research Office [ARO]) for his encouragement and support of this project.

The authors would like to thank Dr. Matthew Biss for his generous help with the experimental setup, Dr. Kevin McNesby, Mr. Gerrit Sutherland, Mr. Stephen Aubert, and Mr. Vincent Boyle for providing critical technical review of the technical report and their thoughtful technical discussion; Mr. Terry Piatt and Ms. Lori Pridgeon for preparing cyclotrimethylene trinitramine (RDX) spherical charges; Mr. Ronnie Thompson, Mr. William Sickels, Mr. Eugene Summers, and Mrs. Deborah Pilarski for their assistance during the small-scale blast testing.

1. Introduction

Traumatic brain injuries (TBI) are frequently caused by blasts, which trigger a series of neuronal biochemical changes, often resulting in reduced brain/nervous system function and/or cell death. These blasts are characterized by 2 phases, an initial positive pressure blast wave, closely followed by a negative pressure phase. The negative pressure shift results in cavitation bubble collapse in the brain and cerebrospinal fluid, and this cavitation is hypothesized as a possible cause for brain injury.¹ Other possible effects of the blast have been suggested, including the stretching or shearing of cell membranes, resulting in axonal disconnection. Diagnosis and classification of TBI for targeted therapies are challenging because of the heterogeneity of TBI.² Hence, understanding blast-induced functional and structural damage effects (at both the cellular and tissue level) at variable timescales after TBI events is critical to rationally linking these mechanically-induced structural changes with measurable effects on brain/nervous system function.

This report describes the experimental approach and preliminary results of applying realistic blast waves to cultured slices of rat hippocampus, a brain region important for higher order brain functions and also distinctly vulnerable to trauma and excitotoxic damage. Hippocampal slice cultures are ideal for studying blast-induced degeneration over an extended recovery period and provide healthy brain tissue with the characteristic neuronal and synaptic organization as found in the adult brain. Hippocampal slices can also serve as models in studying defined blast parameters, with an absence of interpretation problems due to systemic variables.

2. Objective

The objective of the project is to investigate the effects of realistic explosive blast pressure waves on submerged rat hippocampal brain slices using single and/or multiple impacts in water.

3. Experimental Setup

3.1 The Aquarium Setup

A 30.5-cm by 34.5- × 65-cm water-filled polymethylmethacrylate (PMMA) aquarium was used in testing. The thickness of the aquarium wall is 0.2 cm. It was filled with distilled water, maintained at 37 °C with a heating element (Fig. 1). Hippocampal slide inserts were placed

inside a tissue plate and submerged in a Ziploc bag filled with 1 L of warmed, serum-free media (SFM). The Ziploc bag and tissue plates were clamped, secured, and submerged vertically in the middle of the aquarium, 4 inches below the air-water interface (Fig. 2). The aquarium test provides an excellent method for visualization of shockwave movements and their interactions with the cultured tissue slice samples.

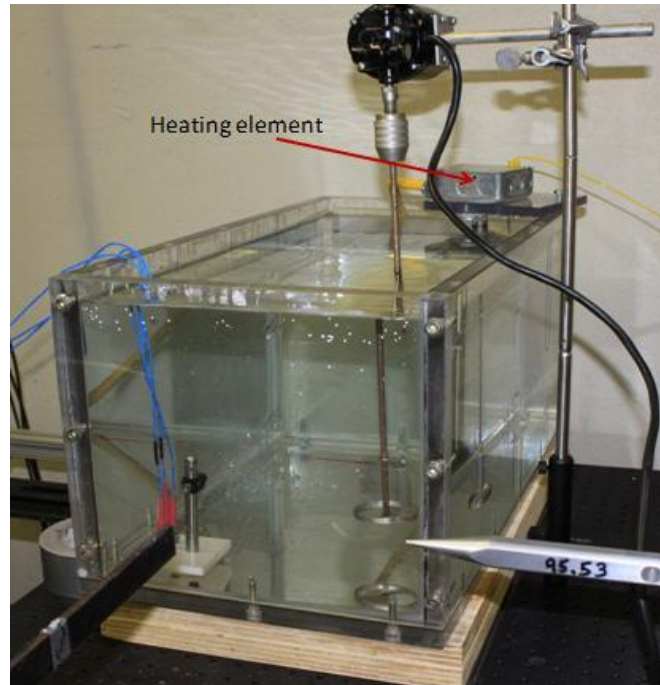


Fig. 1 The aquarium tank

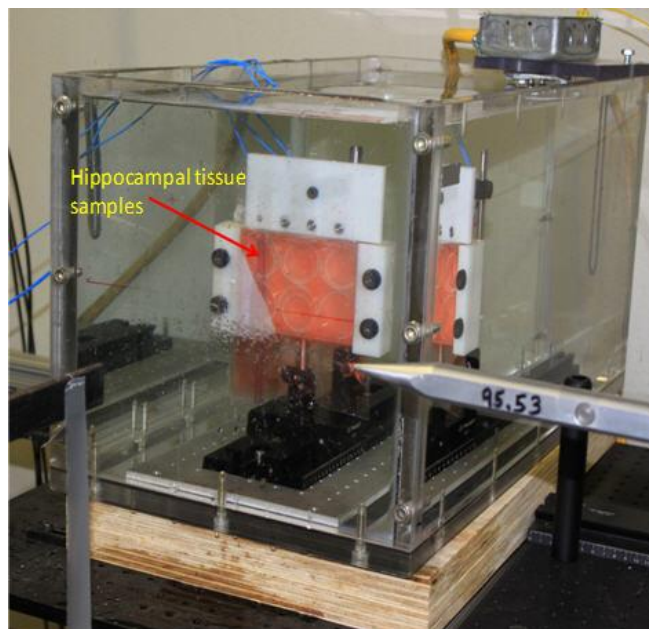


Fig. 2 Cultured tissue samples submerged in the aquarium tank

3.2 Explosive Charges

The 1.7-g cyclotrimethylene trinitramine (RDX) Class 5 spherical charges used in testing were composed of matching hemispherical charges.³ Each hemispherical charge had a nominal mass of 0.85 g, a volume of 0.482 cm³, and was pressed to a density of 1.77 g/cm³ (98.4% theoretical maximum density [TMD]). Figure 3 shows an assembled spherical charge of RDX. Table 1 shows the mass of each experimental hemispherical charge.

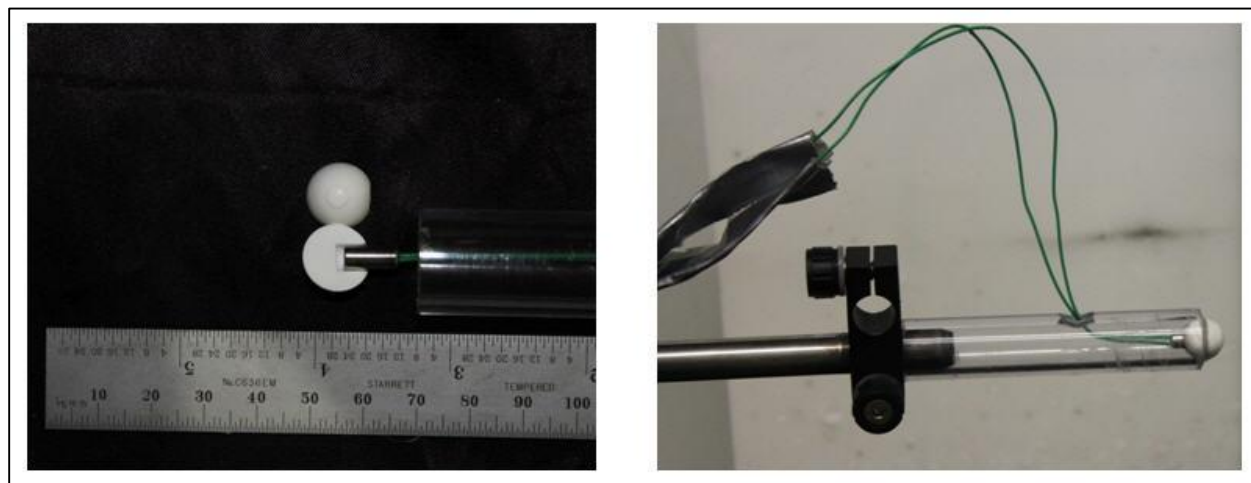


Fig. 3 Spherical RDX charge-matching hemispherical charges (left) and a fully assembled 1.7-g spherical charge (right)

Table 1 Hemispherical charge weight

| Press No. | Mass | Density | TMD |
|-----------|--------|----------------------|-------|
| | (g) | (g/cm ³) | (%) |
| 1 | 0.8541 | 1.771 | 98.36 |
| 2 | 0.8541 | 1.771 | 98.36 |
| 3 | 0.8546 | 1.772 | 98.42 |
| 4 | 0.8540 | 1.770 | 98.35 |
| 5 | 0.8536 | 1.769 | 98.30 |
| 6 | 0.8545 | 1.771 | 98.41 |
| 7 | 0.8541 | 1.771 | 98.36 |
| 8 | 0.8543 | 1.771 | 98.39 |
| 9 | 0.8542 | 1.771 | 98.37 |
| 10 | 0.8535 | 1.769 | 98.29 |
| 11 | 0.8530 | 1.768 | 98.24 |
| 12 | 0.8540 | 1.770 | 98.35 |

3.3 Pressure Sensors and Holder

Three piezoelectric high-frequency dynamic pressure sensors (ICP model 102A, PCB Piezotronics Inc., Depew, NY) were used to measure the shockwave overpressure duration at a position of 2 cm above the cultured samples. All pressure gauges were mounted on top of the tissue sample bag, submerged in the aquarium, and positioned head-on to the blast wave direction (Fig. 4). Two free-field blast pencil probes (ICB model 137A23, PCB Piezotronics Inc., Depew, NY) were positioned in front of the aquarium to measure the free-field blast pressure at a standoff distance of 350 mm before the shockwave entered the water medium (Fig. 5). Pressure-time history traces and peak overpressure were recorded for each blast.

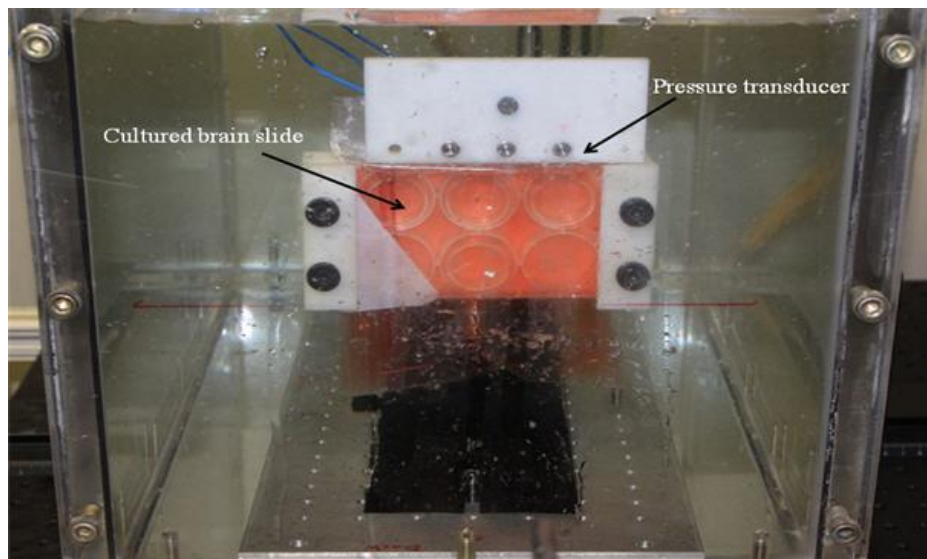


Fig. 4 PCB pressure gauge arrangement

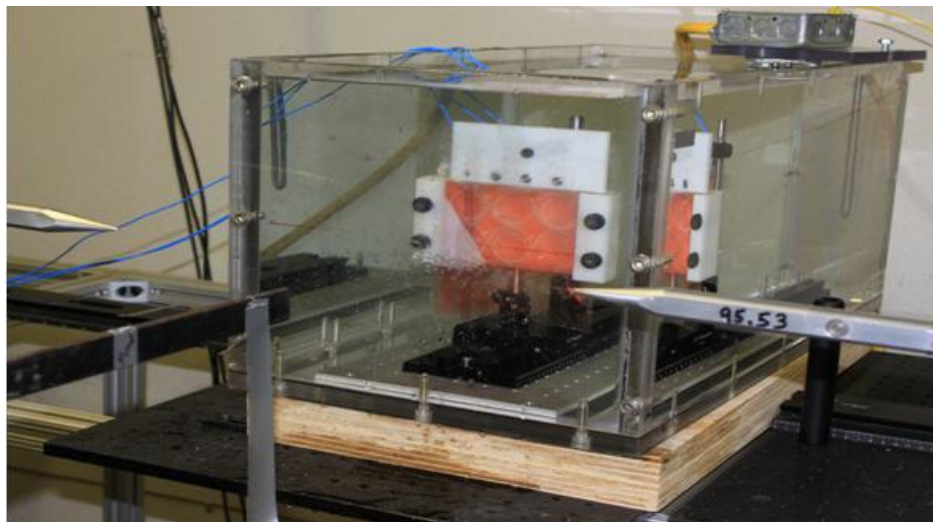


Fig. 5 Free-field pencil gauge arrangement

3.4 Experimental Arrangement

All experiments were conducted at an indoor facility at the US Army Research Laboratory (ARL)-Aberdeen Proving Ground (APG), Maryland. The spherical RDX explosive charge was detonated at 117 cm above the ground using an RP-87 detonator. The charge standoff distance to the cultured tissue sample bag was 350 mm and measured as a clear spacing between the charge and the cultured sample bag (Fig. 6). The standoff distance from the pencil gauge to the RDX sphere was 350 mm. The experimental arrangement is depicted in Fig. 7. High-speed camera images were captured with a resolution of $1,024 \times 64$ pixels using a Photron FASTCAM SA5 Model 1300K-C3 (Photron USA, Inc., San Diego, CA). The camera frame rate was 100,000 frames per second with an exposure time of 368 ns.

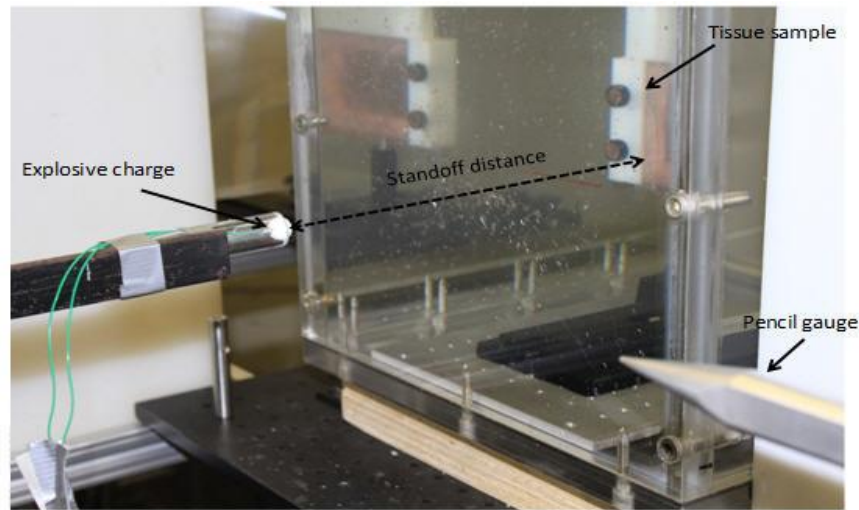


Fig. 6 Explosive charge arrangement

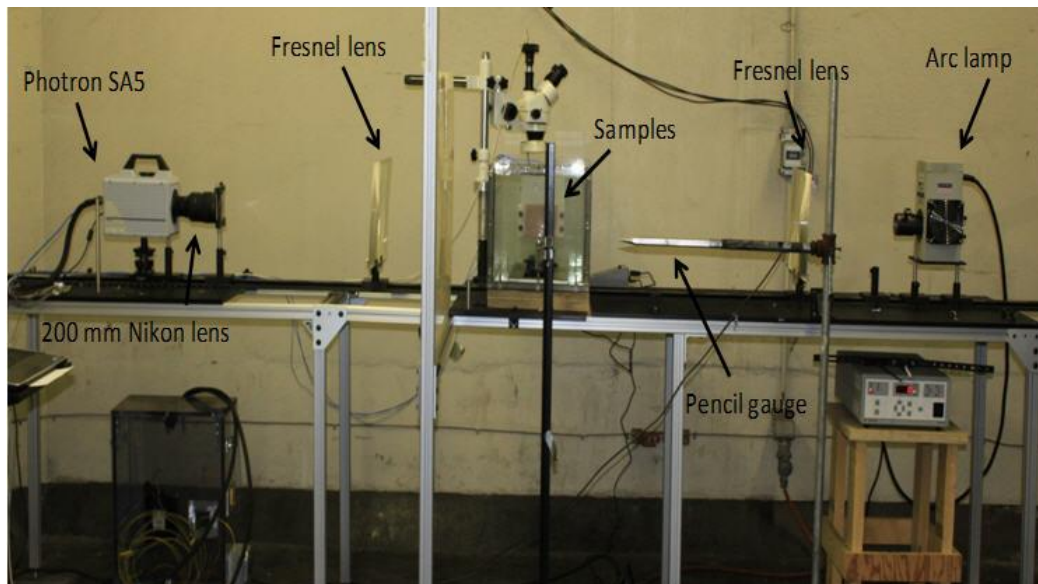


Fig. 7 Experimental arrangement

Figure 8 shows the view from the Photron FastCam SA5 high-speed camera's perspective. The high-speed camera was placed perpendicularly to the sample. The visualization of the blast wave passing through the sample was recorded in a direction perpendicular to the air blast arrival axis with a resolution equal to $1,024 \times 64$.

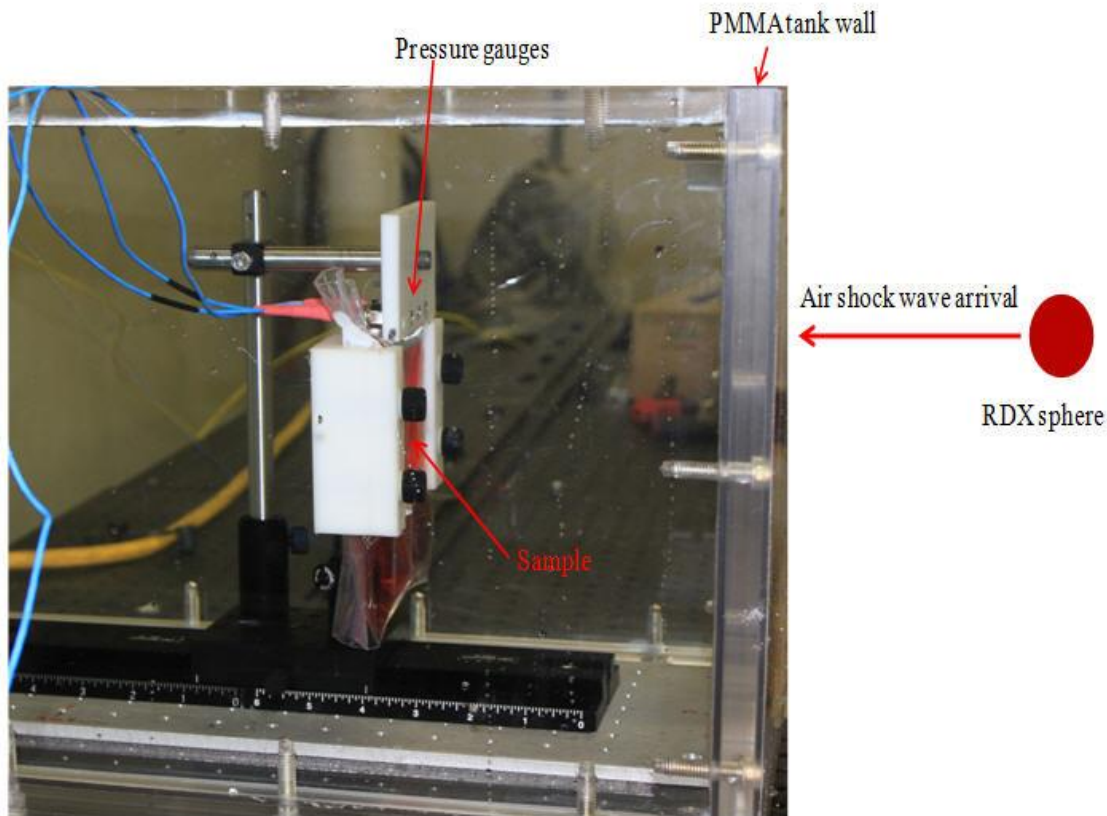


Fig. 8 View from the perspective of the Photron Fastcam SA5 high-speed camera

3.5 Tissue Experimental Procedures

3.5.1 Organotypic Cultures of Hippocampus

Sprague-Dawley Rat Litters (Charles River Laboratories, Wilmington, MA) were housed in accordance with guidelines from the National Institutes of Health. The animals were housed in a temperature and humidity-controlled room with a 12:12-h light–dark cycle, with access to food and water ad libitum. All animal experiments were carried out in compliance with procedures approved by the Institutional Animal Care and Use Committee at the University of North Carolina at Pembroke. Animals at 12 days postnatal age were subjected to isoflurane anesthesia and decapitation, followed by rapid separation of hippocampi in ice-cold holding buffer containing 124-mM sodium chloride (NaCl), 3-mM potassium chloride (KCl), 2-mM calcium chloride (CaCl_2), 4-mM magnesium sulfate (MgSO_4), 1.25-mM monopotassium phosphate (KH_2PO_4), 26-mM sodium bicarbonate (NaHCO_3), 10-mM D-glucose, and 2-mM ascorbic acid.

Transverse slices of hippocampus (400 μm) were then quickly prepared using a McIlwain Mickle tissue chopper and placed in cold holding buffer, followed by gentle positioning of 9 to 10 slices per Millicell-CM insert (shown in Fig. 9). The inserts were placed in 6-well plates (Millipore Corporation, Bedford, MA). After tissue placement, beneath each culture insert was placed 1-ml horse serum-containing media (HSM), composed of 50% basal medium Eagle, 25% Earle's balanced salts, 25% horse serum, and supplemented to the following final concentrations: 136-mM NaCl, 2-mM CaCl_2 , 2.5-mM MgSO_4 , 4-mM NaHCO_3 , 3-mM glutamine, 40-mM glucose, 0.4-mM ascorbic acid, 20-mM HEPES buffer (pH 7.3), 1-mg/l insulin (Sigma Chemical Co., 24 I.U. per mg), 5-units/ml penicillin, and 5-mg/l streptomycin. The prepared slice cultures were supplied with fresh HSM 24 h later (culture day 1) and every 2 to 3 days thereafter while tissue was maintained at 37 °C in 5% CO_2 -enriched and humidified air.

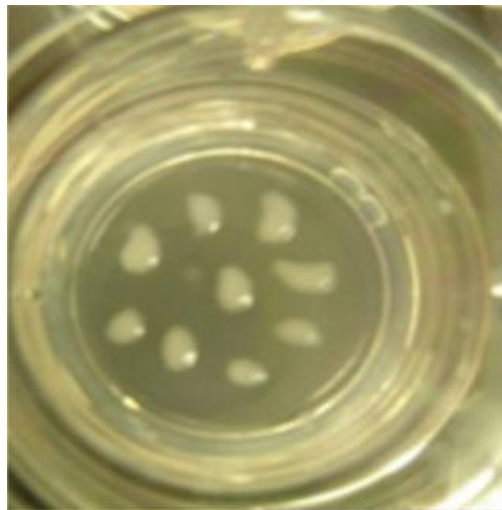


Fig. 9 The organotypic hippocampal slice culture

The slice cultures are typically maintained for a 15- to 20-day maturation period before experiments are initiated. The convenient hippocampal slice culture method provides mature brain tissue exhibiting native neuronal organization and synaptic density as found *in vivo*, thus providing a model to study defined insults and synaptic vulnerability in the absence of systemic variables as shown in previous reports.⁴⁻⁷

3.5.2 Blast Insult Procedure in Hippocampal Slice Cultures

Plates of hippocampal slices at culture day 18 were transported by car for 8 h from Pembroke, North Carolina, to APG, Maryland, while maintained in a sterile, humid, battery-operated tissue incubator. Upon arrival, the plates were placed in a CO_2 incubator at ARL. To deliver a blast insult to a plate containing slice cultures (the blast plate), the lid of the tissue plate was removed and the plate with slice-containing inserts was submerged into a Ziploc bag filled with approximately 1 L of warmed SFM consisting of 50% basal medium Eagle, 25% Earle's balanced salts, 25% HEPES-buffered saline (pH 7.3), and supplemented to the following final concentrations: 136-mM NaCl, 2-mM CaCl_2 , 2.5-mM MgSO_4 , 4-mM NaHCO_3 , 3-mM

glutamine, 40-mM glucose, 0.4-mM ascorbic acid, 1-mg/l insulin (Sigma Chemical Co., 24 I.U. per mg), 5-units/ml penicillin, and 5-mg/L streptomycin. Just prior to submerging the blast plate, a control plate of slices was flooded with warmed SFM to provide tissue with equal submerge time as the blast plate. Positioned next to the flooded control plate, the Ziploc bag containing the blast plate was manipulated in order to remove air bubbles and excess SFM, the bag then sealed and checked for leaks, followed by the bag and tissue plate being positioned vertically into a clamp system (Fig 10). The entire clamp system was then carried to the blast tank in order to place the tissue plate apparatus into the warmed water tank that was then subjected to an external blast event. The control plate of hippocampal slice cultures continued with submerged conditions in a 37 °C incubator while the blast plate was positioned in the 37 °C water bath and received a series of 3 blasts at approximately 4-min intervals. Both plates were then returned to normal culture conditions and supplied with fresh 1-ml aliquots of serum-containing HSM after the common submersion time of 20 min. A second blast plate received a single-blast event and was returned to normal culture conditions after a submersion time of 15 min. All plates were returned to the CO₂ incubator at ARL for the 24–48-h recovery period.



Fig. 10 Cultured brain slice samples submerged in medium ready for testing

3.5.3 Harvesting Hippocampal Slice Samples for Immunoblot Analysis

Groups of 6 to 8 cultured hippocampal slices per sample were gently removed from the Millicell inserts either at 24- or 48-h post-blast time. For the harvesting procedure, the inserts were flooded with ice-cold buffer containing 0.32-M sucrose, 5-mM HEPES (pH 7.5), 1-mM ethylenediaminetetraacetic acid (EDTA), 1-mM ethylene glycol tetraacetic acid (EGTA), protease inhibitors antipain, 4-(2-aminoethyl) benzenesulfonyl fluoride, pepstatin A, E-64, bestatin, leupeptin, and aprotinin (2 µg/ml each). A soft brush was used to release the slices from the insert's Biopore membrane, after which the slices were transferred to centrifuge tubes and quickly pelleted at 3000 rpm for 3 min at 4 °C. The drained tubes were then used to sonicate the

tissue pellets with a fine-tip sonicator on ice, using a small volume of lysis buffer containing 6-mM Tris (pH 8.1), 0.2-mM EDTA, 0.2-mM EGTA, and protease inhibitors. Protein concentrations were determined with the bicinchoninic acid assay (Pierce, Rockford, Illinois) with bovine serum albumin as a standard. Equal amounts of total protein were boiled in sodium dodecyl sulfate (SDS) sample buffer for 5 min, separated by 4%–15% SDS-polyacrylamide gel electrophoresis (PAGE) and transferred to nitrocellulose membranes (Bio-Rad system). The blots were probed with selective antibodies overnight, and then incubated with alkaline phosphatase-conjugated anti-IgG secondary antibodies, and the stained bands visualized with nitro blue tetrazolium/5-bromo- 4-chloro-3-indolyl phosphate colorimetric substrates. The densities of immunoreactive bands were quantified with high-resolution image scanning and BIOQUANT software (R&M Biometrics, Nashville, Tennessee).

4. Results and Discussion

4.1 High-Speed Imaging Record

Figures 11 and 12 show a series of high-speed digital images of the blast pressure waves propagating through the aquarium and impacting the tissue samples. The blast waves were generated from initiation of 1.7 g of RDX sphere in air outside the aquarium.

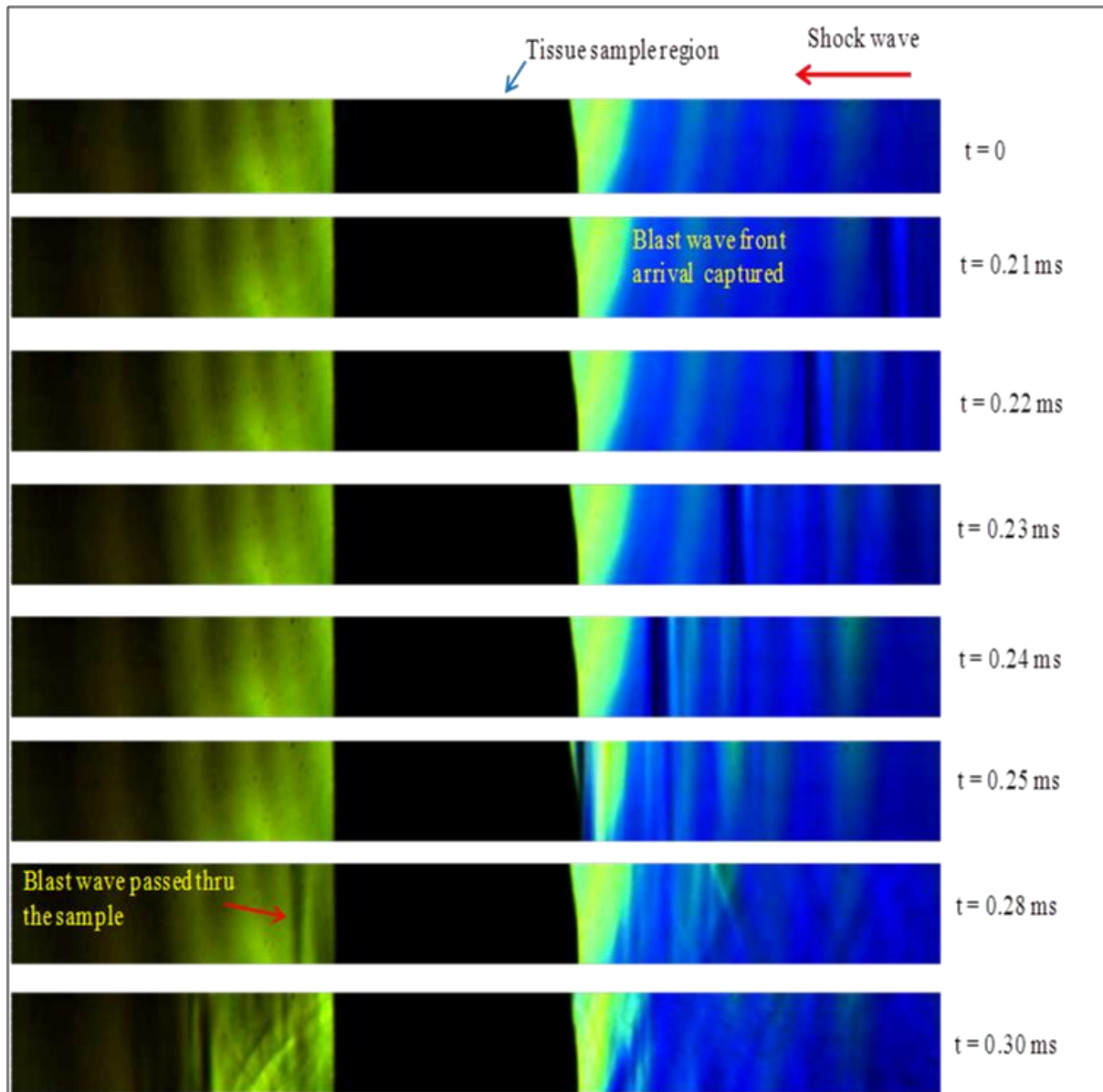


Fig. 11 The blast wave arrival images from $t = 0$ to $t = 0.30 \text{ ms}$

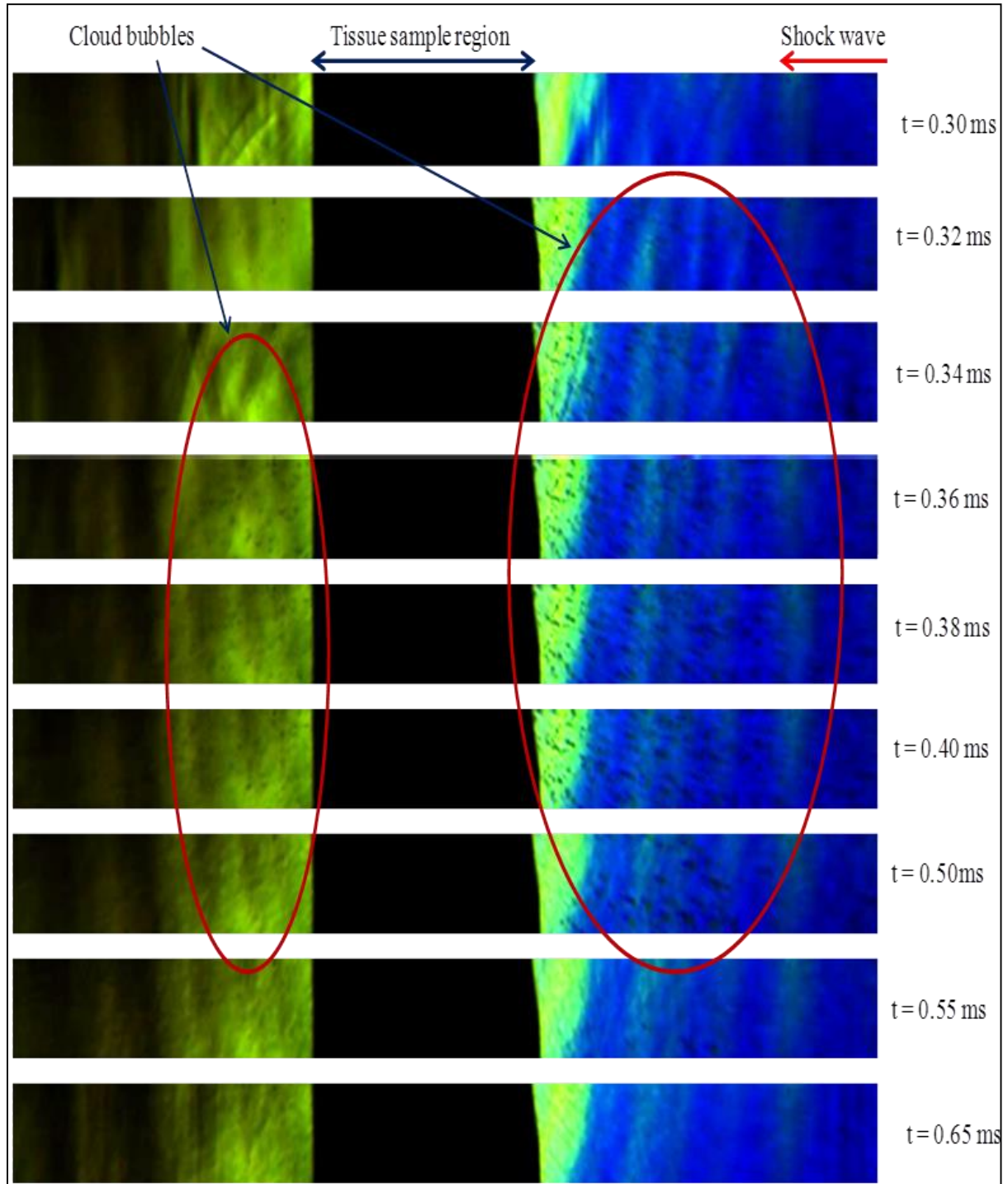


Fig. 12 High-speed images of the blast wave arrival images from $t = 0.30$ ms to $t = 0.65$ ms after the initiation

Figure 11 shows the blast pressure waves propagating from left to right in the aquarium and impacting the tissue samples at 0.21 ms. The impact on the tissue samples produces both transmitted and reflected pressure waves in the aquarium. This is evident at time of 0.30 ms. This

combined complex pressure wave structure produces a yet unexplained bubble cloud possibly due to a cavitation phenomenon.

As shown in Fig. 12, the bubble cloud was captured at approximately 0.32 ms after the initiation. The bubble cloud dissipated completely about 0.6 ms after initiation. It can be seen from these sequences of images that the formation and disappearance of the bubble cloud are within a time span of approximately 0.3 ms. These are typical examples of the bubble cloud formation observed during these explosive blast experiments.

4.2 Experimental Pressure Measurements

Figure 13 illustrates a typical side-on pressure-time history signature observed in air at a 350-mm standoff distance from the point of initiation. As seen in Fig. 13, the pressure rose instantaneously to the peak value of approximately 11 psi, followed by an exponential decay and a second rise in pressure to 5 psi. Following the second pressure rise, the pressure dropped to a negative pressure before returning to zero (ambient) conditions. The pressure profile in Fig. 13 is typical of air blast where the second pressure wave is caused primarily from reflection from the aquarium tank. Figure 14 shows a typical pressure-time history record observed in the water at a 350-mm standoff distance from the point of initiation. The pressure rose instantaneously to the peak value of 97 psi and decreased at a nearly exponential rate. The first pressure spike in both signatures is the leading edge of the blast front and is considered as one of the most important factors in the pathology of primary blast injury. The entire process took place in a few milliseconds.

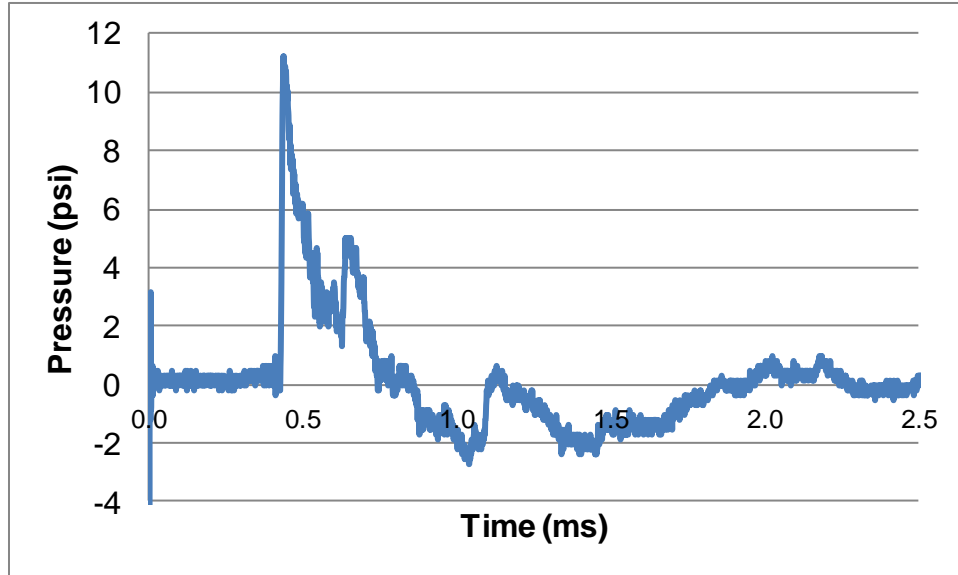


Fig. 13 A typical side-on pressure-time history signature recorded in air

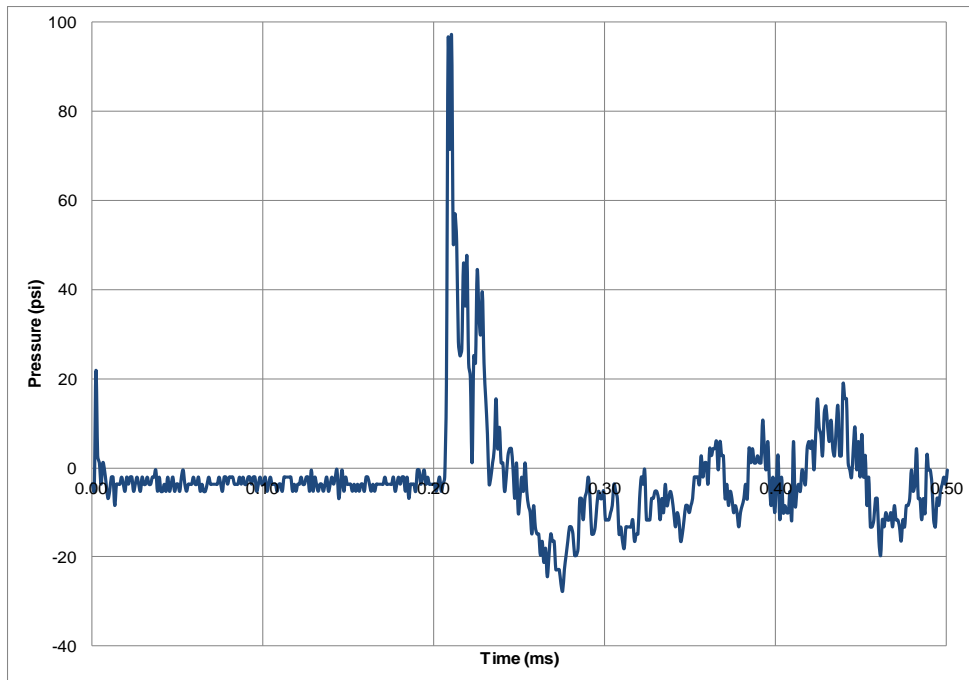


Fig. 14 A typical head-on pressure-time history signature recorded in water

Table 2 shows a summary of the measured peak head-on overpressure produced from pressure sensors placed on the extreme top of the tissue samples. No pressure probes were placed in direct contact with the sealed tissue samples, primarily to prevent both contamination and undue leakage in or out of the tissue sample bags. Simulation and modeling was used (discussed in Section 4.3) to estimate the impact pressures on the tissue slices (see Section 4.3).

Table 2 Peak incident (head-on) experimental pressures inside the tank

| Shot No. | Peak Pressure 1 Transducer No. 1 (psi) | Peak Pressure 2 Transducer No. 2 (psi) | Peak Pressure 3 Transducer No. 3 (psi) |
|----------------------------|--|--|--|
| Single blast (control) | 80.55 | 154 | 175 |
| Single blast (with tissue) | 111.5 | 146.1 | 156.8 |
| Triple blast | ... | ... | ... |
| Shot 1 | 117.88 | 154.03 | 156.74 |
| Shot 2 | 108.7 | 125.37 | 125 |
| Shot 3 | 97.1 | 134.9 | 139.29 |

4.3 Modeling and Simulation of Blast-Generated Pressure

In addition to the aforementioned experimental techniques, blast simulations were also performed using the CTH shock physics code. CTH is an Eulerian shock physics code developed at Sandia National Laboratories, and for these experiments it was used to simulate the generated pressure field profile. In CTH, Adaptive Mesh Refinement (AMR) capabilities were utilized to refine the expanding propagating shock front as it moved through the spatial domain.

Figure 15 shows the problem geometry setup. RDX spherical charges were placed at variable distances of 125 mm and 150 mm directly in front of an aquarium tank with wall thickness of 20 mm. Sample packs were placed in the tank at a fixed distance of 180 mm from the front inside wall. The total combined distances from the charge to the sample for the cases considered were 325 mm and 350 mm respectively.

To simplify the problem geometry, unnecessary items such as stands and clamp holders were neglected. As the explosive detonated in air, AMR refinement techniques were used to resolve the shock front as it propagated from the air medium through the aquarium Poly(methyl methacrylate) (PMMA) material and into the fluid (water) medium. The strength of the pressure waves from the RDX-blast through the PMMA, and subsequently through the water medium, and the sample pack were investigated using strategically placed tracer particles (see Fig. 15).

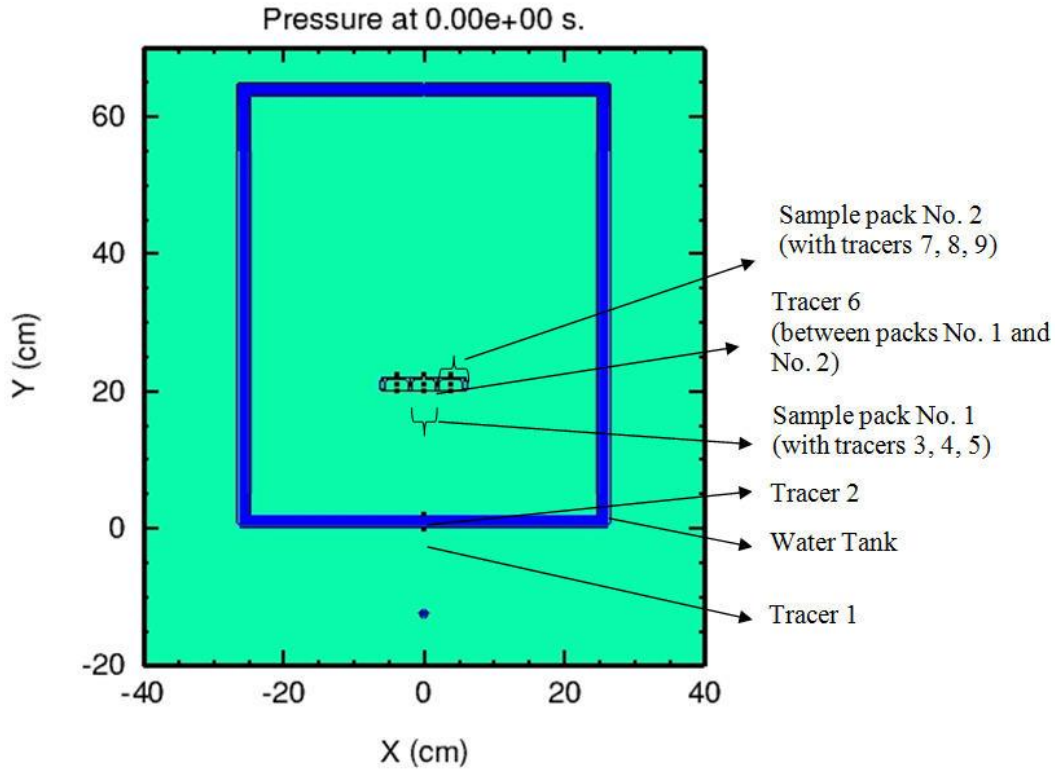


Fig. 15 Numerical blast simulation setup. Test sample packs Nos. 1 and 2 were placed 180 mm from the tank front inner wall. The distances from the RDX charges to the tank front wall were 125 mm and 150 mm, respectively. Tank wall thickness was 20 mm.

Table 3 provides the recorded spatial positions and peak pressures determined from the use of the tracer particles for the case where the RDX charge was placed at 325-mm standoff distance from the tissue slice samples. The strongest pressure waves were recorded at the front of the tank in air (see Table 3, tracer 1). This recording was from the combination of incoming pressure waves and reflected pressure waves from the tank front. As the pressure waves traverse from the air through the PMMA and into the water medium there was a significant decrease in peak pressure (Table 3, tracer 2). This was a result of the impedance mismatch between the PMMA and the water medium. Table 3 highlights the declining strength of the pressure wave impact on the sample pack ranging from 95 psi down to 50 psi (see Table 3 tracers 3–9).

Table 3 Tracer location and peak pressure at 325-mm standoff distance from the charge to the sample

| Tracer No. | Location | Position (cm) | Peak Pressure (psi) |
|------------|---|-----------------------|---------------------|
| 1 | Outside tank front | $x = 0$ $y = -0.1$ | 496.84 |
| 2 | Inside tank front | $x = 0$ $y = 1.91$ | 171.43 |
| 3 | First sample (entrance) | $x = 0$ $y = 19.91$ | 94.99 |
| 4 | First sample (centered) | $x = 0$ $y = 21.0$ | 65.02 |
| 5 | First sample (back wall in water) | $x = 0$ $y = 22.26$ | 56.37 |
| 6 | Mid tracer between samples (positioned in holder) | $x = 1.95$ $y = 21.0$ | 51.43 |
| 7 | Second sample (entrance) | $x = 3.9$ $y = 19.91$ | 51.74 |
| 8 | Second sample (centered) | $x = 3.9$ $y = 21.0$ | 58.05 |
| 9 | Second sample (back wall in water) | $x = 3.9$ $y = 22.26$ | 50.80 |

Table 4 Peak pressures generated by simulation at the entrance, inside and back wall of sample packs

| Sample Packs (No.) | Peak Pressure at Sample Entrance (psi) | Peak Pressure Inside Sample Well (psi) | Peak Pressure at the Back of Sample (psi) |
|--------------------|--|--|---|
| 1 | 121.218 | 84.2332 | 44.5203 |
| 2 | 44.958 | 48.5469 | 45.1331 |

The corresponding pressure contour field distribution from the air blast into the water medium and the interaction with the sample packs at each tracer location is presented in Figs. 16–20. The simulated blast scenario was started with the initiation of a 1.71-g spherical RDX charge 12.3 mm in diameter. The blast wave was permitted to propagate across the PMMA tank as illustrated in Figs. 16a and 17a. Lagrangian tracer particles were placed just ahead (tracer 1) and behind the tank walls (tracer 2). These tracer particles captured the strength of the pressure waves as shown in Figs. 16b and 17b. The results from tracer 1 produced a peak pressure close to 500 psi. As the waves propagated into the water medium their strength dropped significantly as shown in Fig. 17b. Figure 18 shows the later time wave propagation across 3 sample packs that were placed perpendicularly to the direction of flow. This was done deliberately to investigate the pressure profile within the sample wells. The idea here was to increase and acquire knowledge about the wave motion inside the sample wells and determine the structure of the wave profiles, which has proven to be difficult to assess experimentally. An expanded view of the sample packs is shown in Fig. 18 on the right. Sample pack No. 1 is centered while sample packs Nos. 2 and 3 are shown to the right and left respectively. The identifiable tracers 3–9 were used in the investigation.

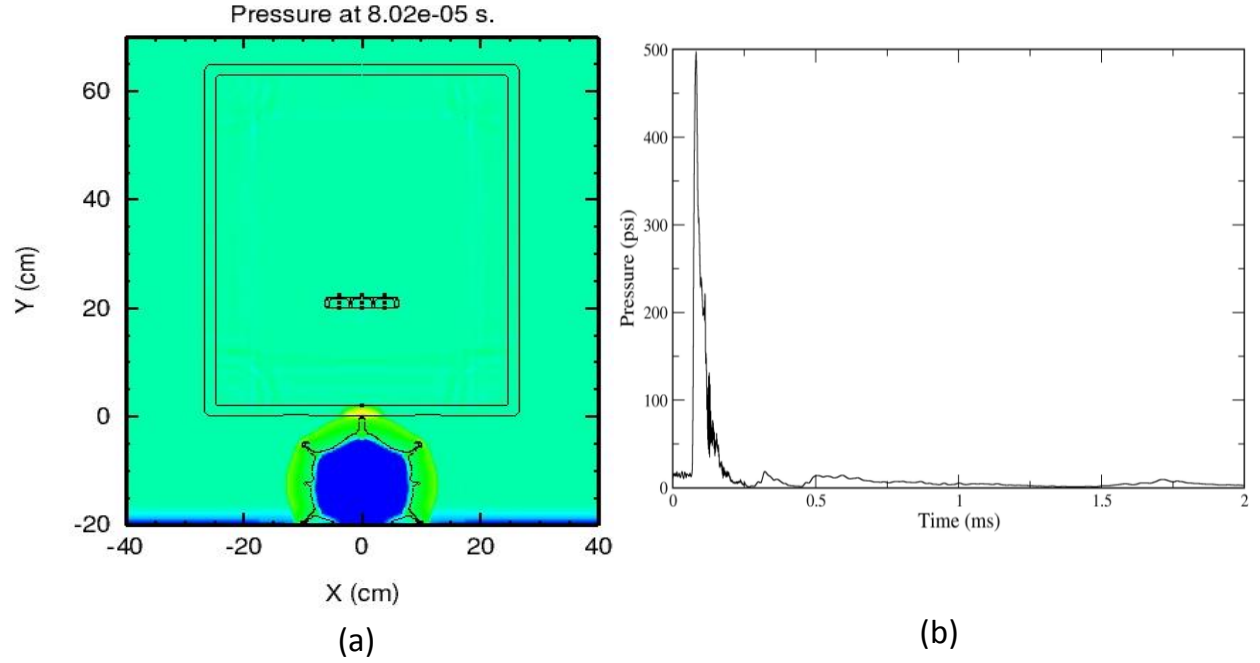


Fig. 16 a) Pressure contours from RDX air blast initiated from standoff distance of 125 mm from tank front wall. b) Pressure history for tracer particle 1 located (0 cm, -0.1cm) on the tank front wall.

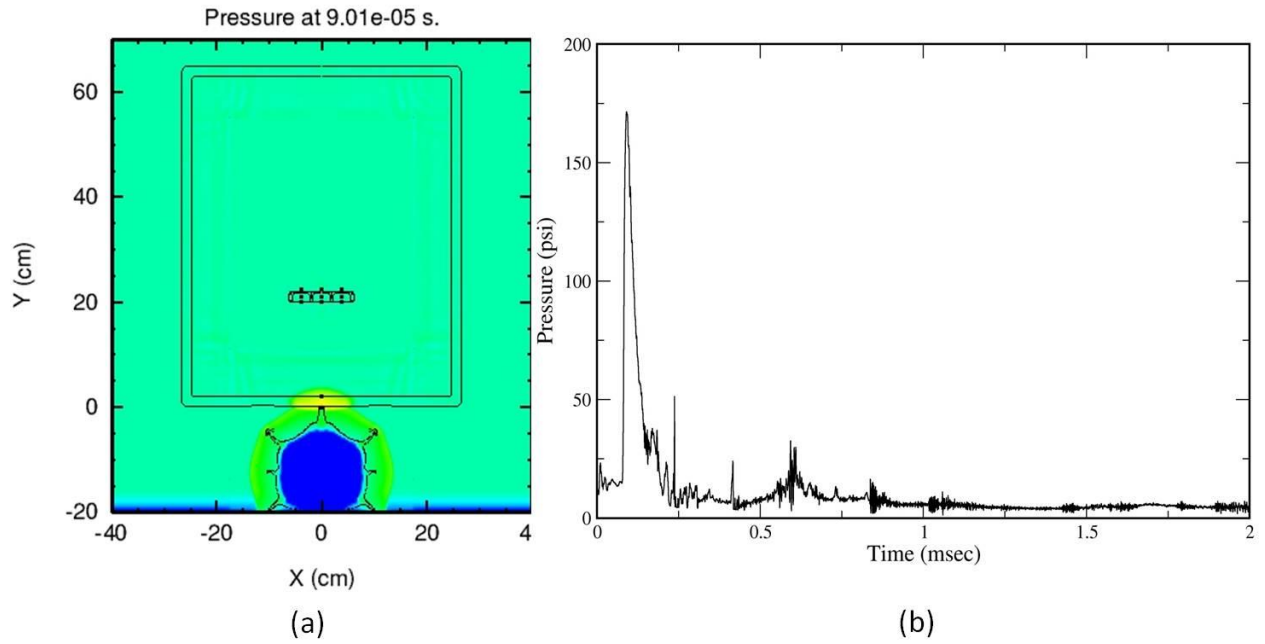


Fig. 17 a) Pressure contours propagating across the tank wall (standoff 125 mm). b) Pressure histories for tracer particle 2 located (0 cm, 1.91 cm) on inner tank wall.

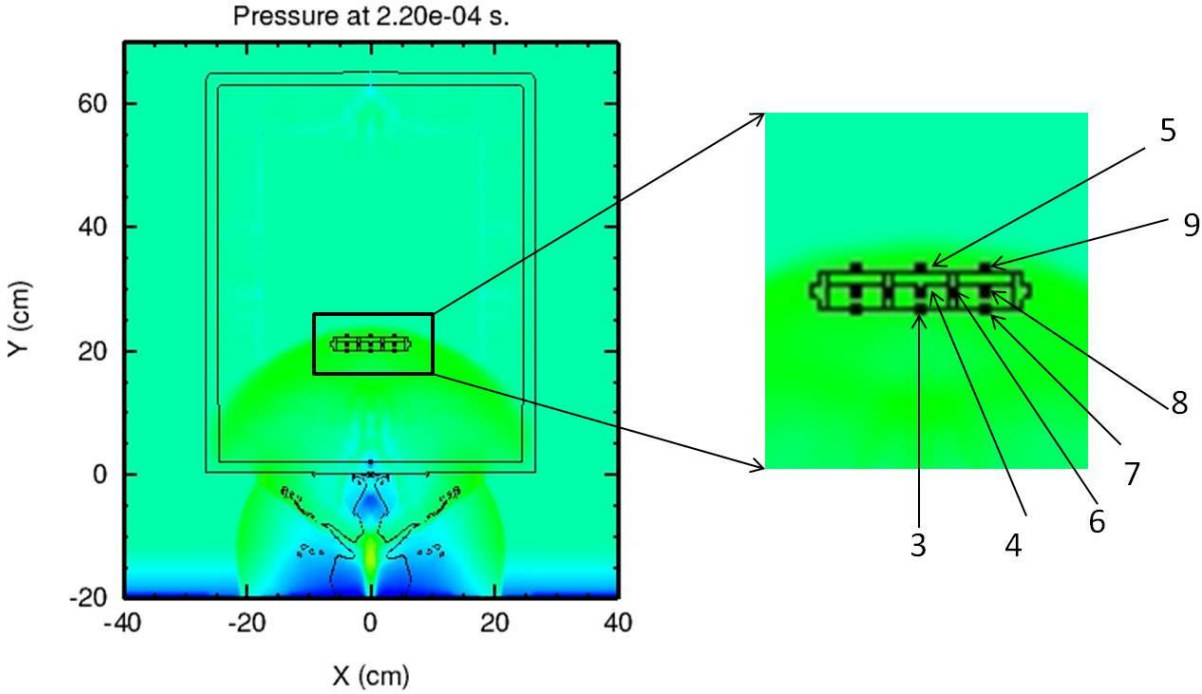


Fig. 18 Pressure waves propagating across the sample packs with tracers 3–9 identified (Initiated standoff 125 mm)

Time-resolved histories of pressure in each sample pack were recorded at the tracer locations. The structure of the pressure waves in the sample packs are illustrated in Figs.19 and 20. Figure 19 shows the comparison of sample pack No. 1 (19a) and 2 (19b). The tracer recording in sample pack No. 1 (Fig. 19a) at the entrance showed an initial pressure rise of 58 psi followed by a stronger reflected pressure at a peak of 95 psi. Inside sample pack No. 1 the pressure continue rise to 65 psi followed by a lower reflected pressure at 55 psi.

Similarly at the entrance sample pack No. 2 (Fig. 19b) an initial pressure recording of 52 psi was followed by a lower reflected pressure at 38 psi. It is interesting to note that the recordings from tracer 4 and tracer 8 inside sample pack No.1 and No.2 respectively show similar pressure history profiles with peak pressures on the order of 65 and 67 psi respectively.

Figures 20a and 20b show the wave structure in the water medium just beyond the back walls of both sample packs Nos. 1 and 2 (tracers 5 and 9, respectively). The peak pressure dropped from 65 psi inside the well to 56 psi in the water medium just beyond sample pack No. 1, while the peak pressure dropped from 58 psi inside the well to 51 psi just beyond sample pack No. 2. A tracer particle was also embedded in the sample holder located between the sample pack No. 1 and sample pack No. 2 (see Fig. 20c, tracer 6). The recorded results revealed low-peak pressures on the order of 50 psi. The recorded result was in line with the results from tracer 9 (Fig. 20b).

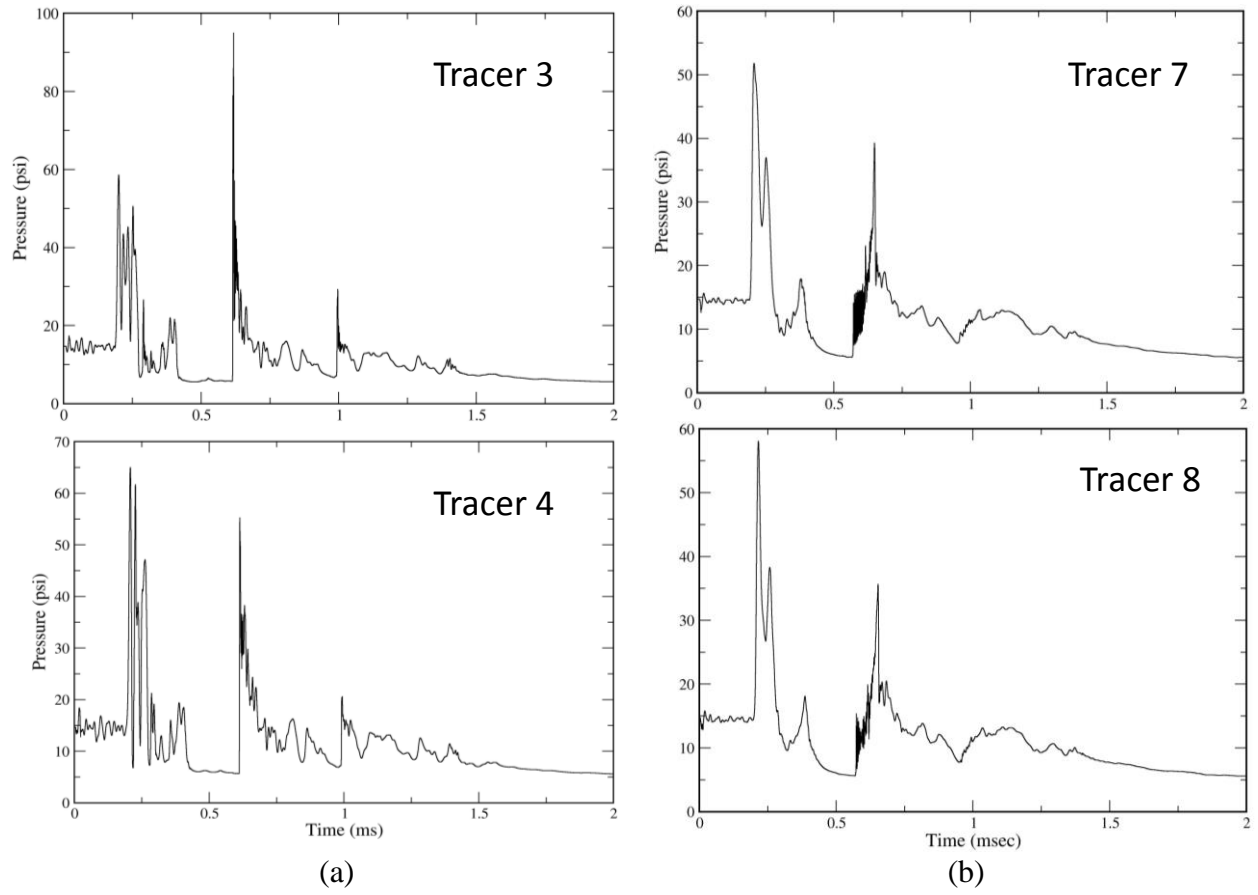


Fig. 19 a) Pressure histories at tracer locations 3 and 4 located in sample pack No. 1; b) pressure histories at tracer locations 7 and 8 located in sample pack No. 2 (standoff distance 125 mm)

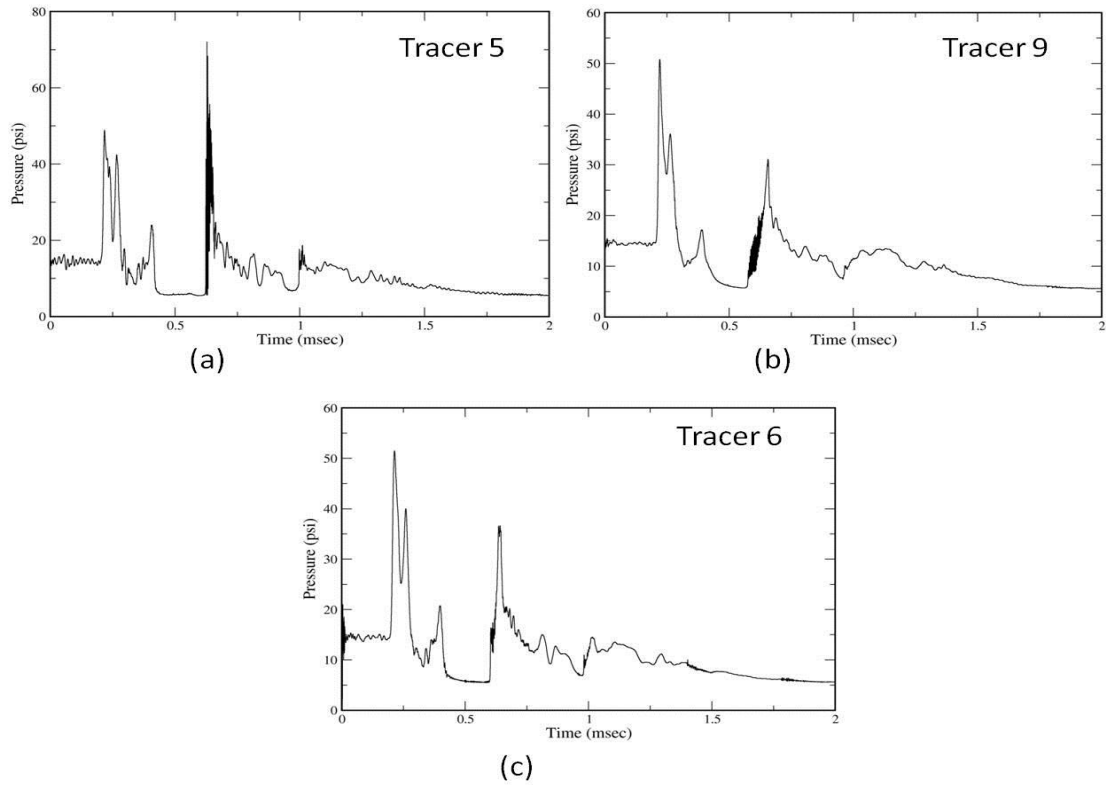


Fig. 20 a) Pressure histories at tracer location 5; b) pressure histories at tracer location 9; c) pressure histories at tracer 6 located between sample packs Nos. 1 and 2. (Standoff 125 mm).

Figure 21 shows the experimental results compared with simulations calculations for the case where the sample packs were removed with only the pressures gauge maintained in the water medium at 325 mm from the RDX charge. A time shift of 0.04 ms was required in the simulation to account for the delayed time in the experimental pressure histories. Nevertheless, both simulations and experiments captured the peak pressures at about 138 psi.

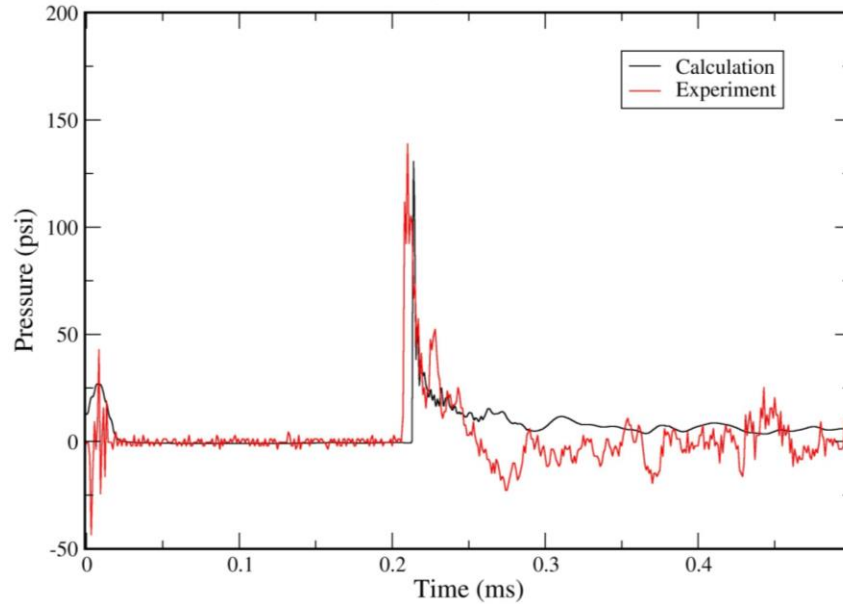


Fig. 21 Comparison of experiment and calculation of pressure-time history signature recorded in water from aquarium experiment

Figure 22 shows the pressure contours from an RDX air-blast propagating across the aquarium front wall and into the sample packs. The RDX explosive was positioned 350 mm away from the sample packs. An expanded view of the pressure contour into the sample packs is shown to the right of Fig. 22 with identifiable tracers 3–9 used to record the pressure histories at the entrance, inside, and outside the back walls of sample packs Nos. 1 and 2. As identified earlier in Fig. 15, tracers 3, 4, and 5 were associated with sample pack No. 1, while tracers 7, 8, and 9 were associated with sample pack No. 2. Tracer 6 was position between both sample packs.

The recorded histories and structure of the profile of the impacting pressures waves on the sample packs are shown in Figs. 23 and 24. Figure 23 shows double impact pressure waves on sample pack No. 1 (Fig. 23a). That is, a peak pressure around 48 psi followed by a reflected wave at 75 psi was exhibited at the entrance (see Fig. 23a tracer 3). Inside the sample pack No. 1 the recording revealed a peak pressure of 52 psi followed by lower reflected shock at 46 psi.

In sample pack No. 2 (Fig. 23b) the entrance impact pressure was recorded at 44 psi followed by a lower reflected pressure of 30 psi (see tracer 7). Inside the sample well, pressure rose slightly to 48 psi followed by a weak reflected pressure on the order of 23 psi.

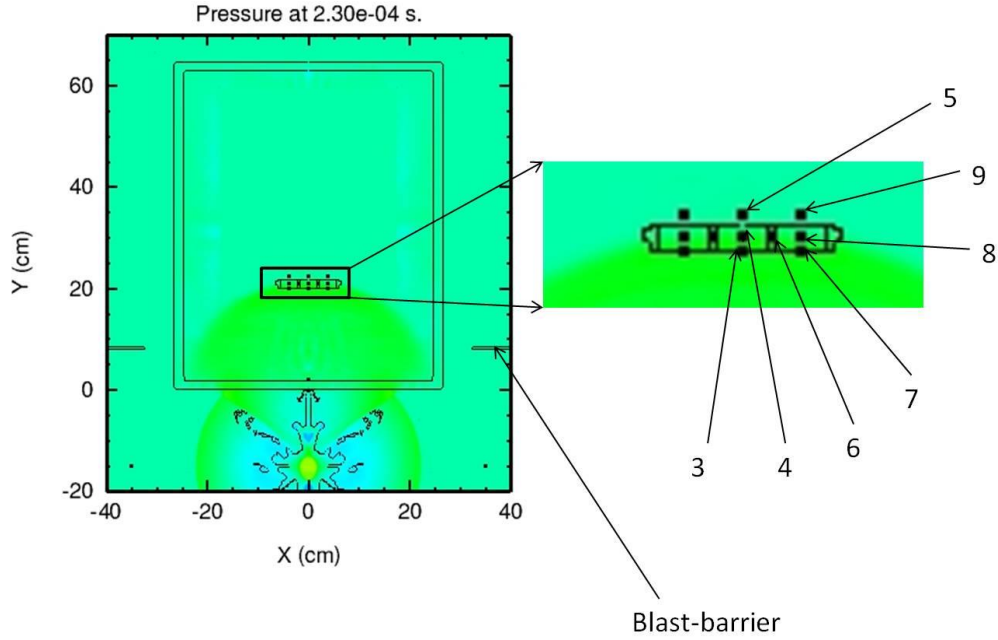


Fig. 22 Pressure waves propagating across the sample packs with tracers 3–9 identified. Explosive standoff was at 150 mm from the front of the aquarium.

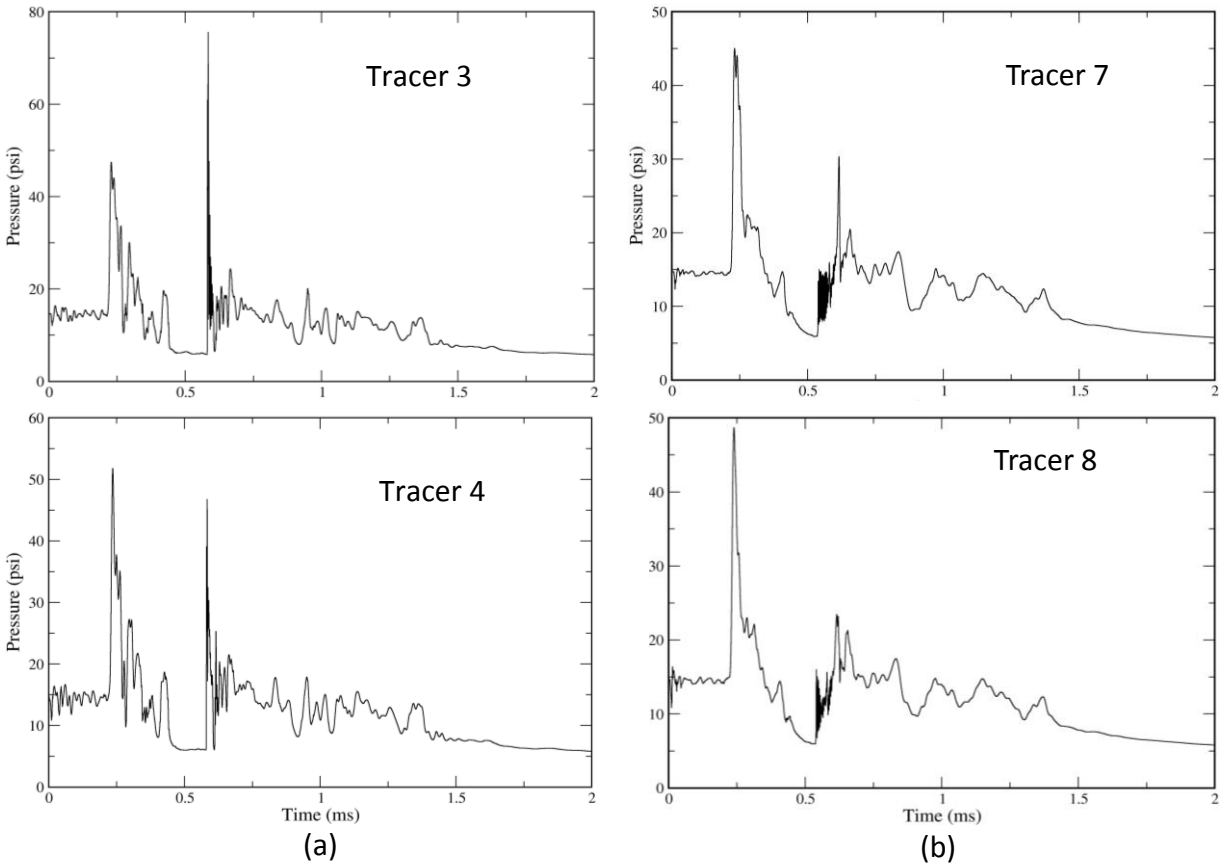


Fig. 23 a) Pressure histories at tracer locations 3 and 4 located in sample pack No. 1; b) pressure histories at tracer locations 7 and 8 located in sample pack No. 2

Figure 24 shows the pressure histories in the water medium just behind the back walls of sample packs Nos. 1 and 2, respectively (see tracers 5 and 9). Tracer 6 shows the pressure histories between both sample packs. Based on the results shown, the structure of the pressure waves was similar in all 3 cases. The peak recorded pressures in these cases were on the order of 45 psi, followed by dying pressure waves. Table 4 summarized the recorded pressures obtained from the numerical simulations at the sample packs entrance, inside and just behind the sample packs back wall.

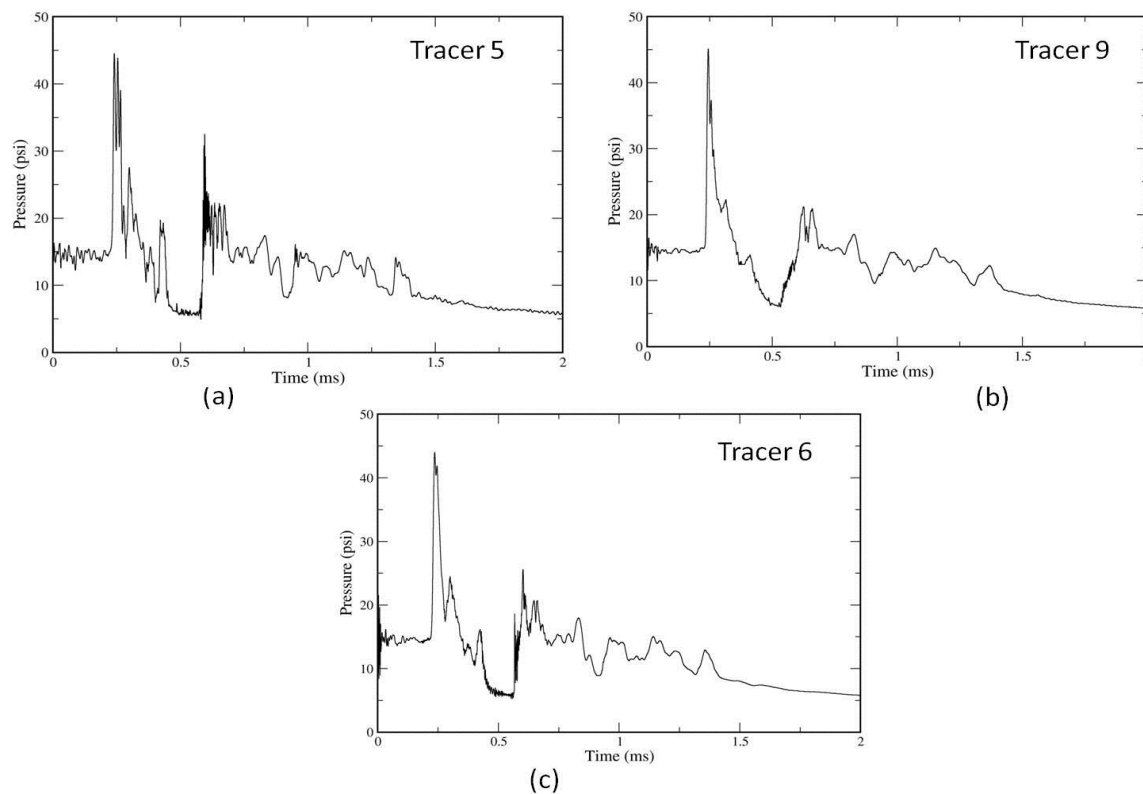


Fig. 24 a) Pressure histories at tracer location 5; b) pressure histories at tracer location 9; c) pressure histories at tracer 6 located between sample packs Nos. 1 and 2

4.4 Assessment of the GluR1 Synaptic Marker in 48-h Post-Blast Samples

Hippocampal slice cultures were submerged in SFM for 20 min (submerge control) or were submerged either for the same 20-min period during which time the slices were subjected to either a series of 3 blasts in the gun room's water tank (at approximately 4-min intervals between each blast), or a single blast detonated outside the aquarium tank. All brain slices were returned to normal culture conditions for 48-h post blast, gently harvested in groups of 6 to 8 slices, followed by homogenization in order to assess blot samples of equal protein per lane for the postsynaptic marker GluR. Reduction of GluR1 synaptic markers is characteristic of synaptic

compromise or synaptotoxicity. Equal protein aliquots were loaded for SDS-PAGE separation, and the postsynaptic marker GluR1 was labeled with antibodies made against its carboxy-terminal domain Ser-His-Ser-Ser-Gly-Met-Pro-Leu-Gly-Ala-Thr-Gly-Leu and affinity purified on the immobilized peptide. Development of immunoreactive proteins was terminated before maximal intensity was reached in order to avoid saturation, and bands were scanned at high resolution to determine integrated optical density values. As shown in Fig. 25, hippocampal slices subjected to a triple blast insult exhibited a 76% reduction in the GluR1 synaptic marker as compared to control slices subjected to equal submersion time of 20 min. Note that, in samples also harvested 48 h after the blast procedure, a single blast had no effect on GluR1 levels (mean integrated density \pm standard error of the mean (SEM), (see Fig. 25). The small upward trend in the single-blast slices is within the variance range of GluR1 levels, or could be related to the fact that the single-blast procedure had a shorter submersion time (15 min versus 20 min).

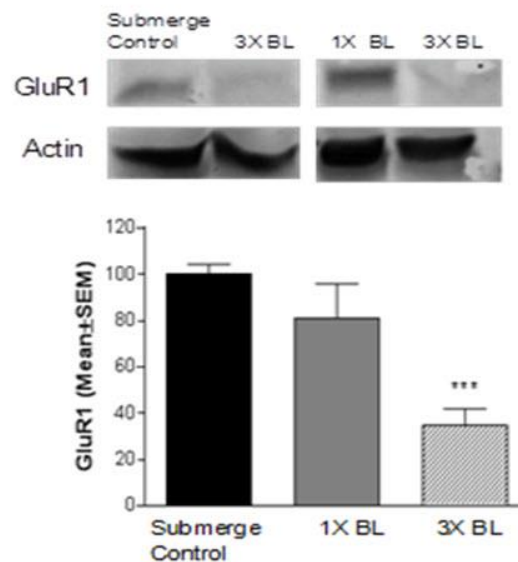


Fig. 25 GluR1 is markedly reduced in response to a triple blast insult. OHSC's exposed to a single blast insult did not demonstrate a change in the post-synaptic marker GluR1. Triple blast shockwaves greatly reduced the level of GluR1. ANOVA $p=0.0009$ (Posthoc test *** ($p < 0.001$)).

5. Summary

These initial studies on blast-induced neurodegeneration in brain slice samples were conducted by using a novel *in vitro* indoor explosively-generated blast impact experimental system to probe the effects of explosive blast (ranging from about 20 to 100 psi) on cultured tissue slice samples.

The initial results showed that a single blast had no effect on the GluR1 immunoreactivity level, whereas the triple blast insult caused a significant reduction in the GluR1 synaptic marker compared to the submerged control slices. This might be an indication of a dose-dependent effect. These results warrant further analysis of hippocampal slice samples to better understand dose-dependent effects of blast-induced brain damage. Slices harvested earlier and later during the recovery period will provide more information concerning the onset of neurodegeneration and injury thresholds and thus determining whether distinct stages of blast-induced injury occur, as well as blast threshold profiles for induction of transient changes versus induction of persistent cellular damage. Subsequent analyses will assess whether cytoskeletal deterioration and/or loss of presynaptic integrity contribute to the damage, providing additional indicators of blast-induced neuronal compromise.

Based on the recorded tracer data and the simulated pressure wave propagation, the most effective peak pressures were determined along the center line location of the tank. As the pressure wave diverged outward from the air blast, the pressure wave weakened. The wave propagation from air-to-PMMA produced a short rise in pressure, followed by a drop in peak pressure in the transition from PMMA-to-water. The confined sample packs Nos. 1 and 2 produced slightly elevated pressures. However, with controlled standoff distances and knowledge of the explosive strength, the desired input pressures in the samples can be determined and controlled. The internal interactions in the sample wells still need further investigation. More advanced 3-dimensional simulations are desirable as well. Current efforts are underway to pursue this line of investigation and to extend our knowledge in investigating the influence of pressure wave impact on neuronal cells.

6. References

1. Goeller J, Wardlaw A, Treichler D, O'Bruba J, Weiss G. Investigation of cavitation as a possible damage mechanism in blast-induced traumatic brain injury. *J Neurotrauma*. 2012;29(10):1970–81.
2. Saatman K, Duhaime A, Bullock R, Maas A, Valadka A, Manley G. Classification of traumatic brain injury for targeted therapies. *J Neurotrauma*. 2008;25:719–738.
3. Biss M. Removing full-scale testing barriers: energetic material detonation characterization at the laboratory scale. Aberdeen Proving Ground (MD): Army Research Laboratory (US); 2012 March. Report No.: ARL-TR-5943. Also available at http://www.arl.army.mil/www/default.cfm?technical_report=6386
4. Bahr BA. Long-term hippocampal slices: a model system for investigating synaptic mechanisms and pathologic processes. *J Neurosci Res*. 1995;42:294–305.
5. Bahr BA. Integrin-type signaling has a distinct influence on NMDA-induced cytoskeletal disassembly. *J. Nuerosci Res*. 2000;59:827-832.
6. Karanian DA, Baude A, Brown QB, Parsons C, Bahr BA. 3-Nitropropionic acid toxicity in hippocampus: Protection through N-methyl-D-aspartate receptor antagonism. *Hippocampus*. 2006;16:834-842.
7. Wisniewski ML, Hwang J, Bahr BA. Submicromolar A β 42 reduced hippocampal glutamate receptors and presynaptic markers in an aggregation-dependent manner. *Biochim Biophys Acta (Mol. Basis of Disease)*. 2011;1812:1664-1674.

List of Symbols, Abbreviations, and Acronyms

| | |
|---------------------------------|--|
| AMR | Adaptive Mesh Refinement |
| ARL | U.S. Army Research Laboratory |
| APG | Aberdeen Proving Ground |
| ARO | Army Research Office |
| CaCl ₂ | calcium chloride |
| DSI | Director's Strategic Initiatives |
| EDTA | ethylenediaminetetraacetic acid |
| EGTA | ethylene glycol tetraacetic acid |
| HSM | horse serum-containing media |
| KCl | potassium chloride |
| KH ₂ PO ₄ | monopotassium phosphate |
| MgSO ₄ | magnesium sulfate |
| NaCl | sodium chloride |
| NaHCO ₃ | sodium bicarbonate |
| PAGE | polyacrylamide gel electrophoresis |
| PMMA | polymethylmethacrylate |
| RDECOM | U.S. Army Research Development and Engineering Command |
| RDX | cyclotrimethylene trinitramine |
| SDS | sodium dodecyl sulfate |
| SEM | standard error of mean |
| SFM | serum-free media |
| TBI | traumatic brain injuries |
| TMD | theoretical maximum density |

1 DEFENSE TECHNICAL
(PDF) INFORMATION CTR
DTIC OCA

2 DIRECTOR
(PDF) US ARMY RESEARCH LAB
RDRL CIO LL
IMAL HRA MAIL & RECORDS MGMT

1 GOVT PRINTG OFC
(PDF) A MALHOTRA

6 DIR USARL
(PDF) RDRL WML C
S AUBERT
R BENJAMIN
T PIEHLER
R SPARKS
RDRL WMP G
R BANTON
RDRL WMM G
L PIEHLER